AIMS Mathematics, 10(11): 26168–26186.
DOI: 10.3934/math.20251152
Received: 20 September 2025
Revised: 15 October 2025
Accepted: 05 November 2025
Published: 12 November 2025

https://www.aimspress.com/journal/Math

Research article

Qualitative study of the (2+1)-dimensional BLMPE equation: Variational principle, Hamiltonian and diverse wave solutions

Kangjia Wang*, Kanghua Yan, Feng Shi*, Geng Li and Xiaolian Liu

School of Physics and Electronic Information Engineering, Henan Polytechnic University, Jiaozuo 454003, China

* **Correspondence:** Email: konka05@163.com; sfhpu@outlook.com.

Abstract: The current study aims to present detailed qualitative and quantitative research on the (2+1)-dimensional Boiti-Leon-Manna-Pempinelli equation (BLMPE), which plays a key role in the field of incompressible fluids. First, we constructed the variational principle using the semi-inverse method (SIM) and developed the Hamiltonian based on the variational principle. Then, we derived the planar dynamical system (PDS), depicted the phase portraits, and carried out the bifurcation analysis to expound the existence of wave solutions with the different wave shapes. In addition, chaotic behaviors were elaborated by imposing the perturbed term, and the sensitivity analysis was conducted by taking the different initial conditions. Finally, the invariant algebraic curve approach (based on the PDS), the direct mapping method (from the unified equation), and the Hamiltonian based method were used to investigate the diverse wave solutions, including the anti-kink solitary, kink solitary, periodic, and singular periodic wave solutions. The profiles of these different solutions are graphically illustrated by assigning reasonable parameters. The results of this paper are novel and can provide a better insight into the dynamics of the equation under consideration.

Keywords: chaotic pattern; phase portrait; sensitivity analysis; bifurcation; Hamiltonian; invariant algebraic curve approach
Mathematics Subject Classification: 35C07, 34C23

1. Introduction

Nonlinear partial differential equations (NPDEs), as an important branch of modern

mathematics, occupy an important position in optics [1,2], biology [3,4], fluid dynamics [5,6], and other fields. Constructing the exact analytical and approximate solutions for NPDEs has become crucial, as these solutions can provide profound explanations for the physical model itself, and be used to predict the evolution process of actual physical states, verify the correctness and accuracy of numerical calculation results. Distinguishing the quality of numerical methods can provide inspiration for qualitative research; therefore, the most ideal approach is to obtain explicit analytical expressions (in finite or infinite series form) or some physically meaningful special solutions (such as solitary wave solutions, traveling wave solutions, elliptic function solutions, periodic wave solutions) for various definite solution problems of NPDEs [7–9]. Exact and approximate solutions of NPDEs can provide strong basis for the exploration of qualitative properties of these equations. Moreover, through the exact solution, we can establish mathematical models and derive new discoveries and scientific predictions. Therefore, studying the solutions of NPDEs is very meaningful. Up to date, many different powerful techniques have been presented to solve the NPDEs, e.g., the (G'/G)-expansion method [10,11], transformed rational function approach [12], Bäcklund transformation technique [13,14], general integral method [15,16], tanh-function technique [17,18], exp-function method [19,20], trial equation approach [21,22], Hirota bilinear approach [23,24], extended F-expansion technique [25,26], Darboux transformation [27,28], Riccati equation approach [29,30], bilinear neural network method [31,32] and many others [33,34]. In this work, we will probe the (2+1)-dimensional BLMPE equation as [35–37]

$$U_{xxxy} - 3U_{xx}U_y - 3U_xU_{xy} + U_{yt} = 0, \tag{1}$$

where $U \equiv U(x,y,t)$. Eq (1) can be used to model the (2+1) dimensional interaction between Riemann waves propagating along the y-axis and long waves propagating along the x-axis. In [36], the periodic-wave solutions were explored. In [37], the stair and step soliton wave solutions were studied. In [38], the N-solitons and soliton molecules solutions were studied. In [39], the authors explored the Pfaffian solutions. In [40], the soliton solutions of *Y*-shape were explored. In [41], the diverse travelling wave solutions were extracted. In [42], the Wronskian determinant solutions were obtained. In this research, we will study Eq (1). The structure of this paper is organized as follows: In Section 2, the variational principle (VP) and Hamiltonian are developed. In Section 3, the PDS is derived, and the qualitative analysis is presented. In Section 4, the invariant algebraic curve (IAC) approach, direct mapping method (DMM), and Hamiltonian based method (HBM) are employed to develop the diverse wave structures. In Section 5, the shapes of the obtained exact solutions are presented. Finally, the conclusion is given in Section 6.

2. The VP and Hamiltonian

To look for the VP and Hamiltonian, we bring in the travelling wave transformation as

$$U(x,y,t) = \psi(\vartheta), \vartheta = mx + ny + \omega t. \tag{2}$$

In the above equation, m, n, and ω stand for the non-zero real constants. Using Eq (2), Eq (1) can be converted into the following form

$$m^3 n\psi^{(4)} - 6m^2 n\psi'\psi'' + n\omega\psi'' = 0, \tag{3}$$

which is

$$\psi^{(4)} - \frac{6}{m}\psi'\psi'' + \frac{\omega}{m^3}\psi'' = 0, \tag{4}$$

Where

$$\psi^{(4)} = \frac{d^4\psi}{d\vartheta^4}, \ \psi'' = \frac{d^2\psi}{d\vartheta^2}, \ \psi' = \frac{d\psi}{d\vartheta}.$$

Integrating it once and letting the integration constant as zero, we get

$$\psi''' - \frac{3}{m}(\psi')^2 + \frac{\omega}{m^3}\psi' = 0. \tag{5}$$

Letting

$$\psi' = \Phi. \tag{6}$$

We have

$$\Phi'' - \frac{3}{m}\Phi^2 + \frac{\omega}{m^3}\Phi = 0. \tag{7}$$

By the SIM, its VP can be developed as [43,44]

$$J(\Phi) = \int_0^\infty \left\{ \frac{1}{2}(\Phi')^2 + \frac{1}{m}\Phi^3 - \frac{\omega}{2m^3}\Phi^2 \right\} d\vartheta, \tag{8}$$

which can be expressed as

$$\begin{aligned} J(\Phi) &= \int_0^\infty \left\{ \frac{1}{2}(\Phi')^2 + \frac{1}{m}\Phi^3 - \frac{\omega}{2m^3}\Phi^2 \right\} d\vartheta \\ &= \int_0^\infty \{D - L\} d\vartheta \end{aligned}, \tag{9}$$

where D and L represent the system's kinetic and potential energy, respectively, as

$$D = \frac{1}{2}(\Phi')^2, \tag{10}$$

and

$$L = -\frac{1}{m}\Phi^3 + \frac{\omega}{2m^3}\Phi^2. \tag{11}$$

So, the system's Hamiltonian is found to be

$$\mathrm{H} = D + L = \frac{1}{2}(\Phi')^2 - \frac{1}{m}\Phi^3 + \frac{\omega}{2m^3}\Phi^2. \tag{12}$$

3. Qualitative analysis

This section aims to present the qualitative analysis of the PDS.

3.1. Phase portrait and bifurcation analysis

Based on Eq (7) and the Hamiltonian in Eq (12), we derive the PDS as

$$\begin{cases} \dfrac{d\Phi}{d\vartheta} = \phi \\ \dfrac{d\phi}{d\vartheta} = \varsigma_1 \Phi(\vartheta) + \varsigma_2 \Phi^2(\vartheta) \end{cases}, \tag{13}$$

where

$$\varsigma_1 = -\frac{\omega}{m^3}, \quad \varsigma_2 = \frac{3}{m}. \tag{14}$$

Obviously, we get two equilibrium points as

$$u_0 = (0,0), \quad u_1 = \left(-\frac{\varsigma_1}{\varsigma_2}, 0\right). \tag{15}$$

By Eq (13), we have

$$f'(\Phi) = 2\varsigma_2 \Phi(\vartheta) + \varsigma_1. \tag{16}$$

The Jacobi matrix is

$$J(u_i, 0) = \begin{pmatrix} 0 & 1 \\ 2\varsigma_2 \Phi + \varsigma_1 & 0 \end{pmatrix}. \tag{17}$$

The determinant is

$$Det(J(u_i)) = |J(u_i)| = \begin{vmatrix} 0 & 1 \\ 2\varsigma_2 \Phi + \varsigma_1 & 0 \end{vmatrix} = -2\varsigma_2 \Phi - \varsigma_1. \tag{18}$$

Additionally, we have

I: The point u_i is the center point for $|J(u_i)| > 0$.

II: The point u_i is the saddle point for $|J(u_i)| < 0$.

III: The point u_i is the cusp point for $|J(u_i)| = 0$.

Then, we have:

Case 1: If $\varsigma_1 > 0$ and $\varsigma_2 > 0$, we have $|J(u_0)| = -\varsigma_1 < 0$ and $|J(u_1)| = \varsigma_1 > 0$, thus u_0 belongs to the saddle point, and u_1 is the center point. The phase portrait of this case is displayed in Figure 1(a), we assign $m = 1$, $\omega = -3$. Obviously, the points u_0 $(0,0)$ and u_1 $(-1,0)$ are the saddle and center points, respectively.

Case 2: If $\varsigma_1 > 0$ and $\varsigma_2 < 0$, there are $|J(u_0)| = -\varsigma_1 < 0$ and $|J(u_1)| = \varsigma_1 > 0$, thus u_0 and u_1 are the saddle and center points, respectively. Figure 1(b) unveils the phase portrait for u_0 $(0,0)$ and

u_1 $(1,0)$ with $m=-1$, $\omega=3$.

Case 3: If $\varsigma_1<0$ and $\varsigma_2>0$, then we have $|J(u_0)|=-\varsigma_1>0$ and $|J(u_1)|=\varsigma_1<0$, thus the points u_0 and u_1 belong to the center and saddle points, respectively. The phase portrait for u_0 $(0,0)$ and u_1 $(1,0)$ is presented in Figure 1(c) for $m=1$, $\omega=3$.

Case 4: If $\varsigma_1<0$ and $\varsigma_2<0$, we can find $|J(u_0)|=-\varsigma_1>0$ and $|J(u_1)|=\varsigma_1<0$, so the u_0 and u_1 belongs to the center point and saddle point, respectively. The phase portrait is presented in Figure 1(d) for $m=-1$, $\omega=-3$.

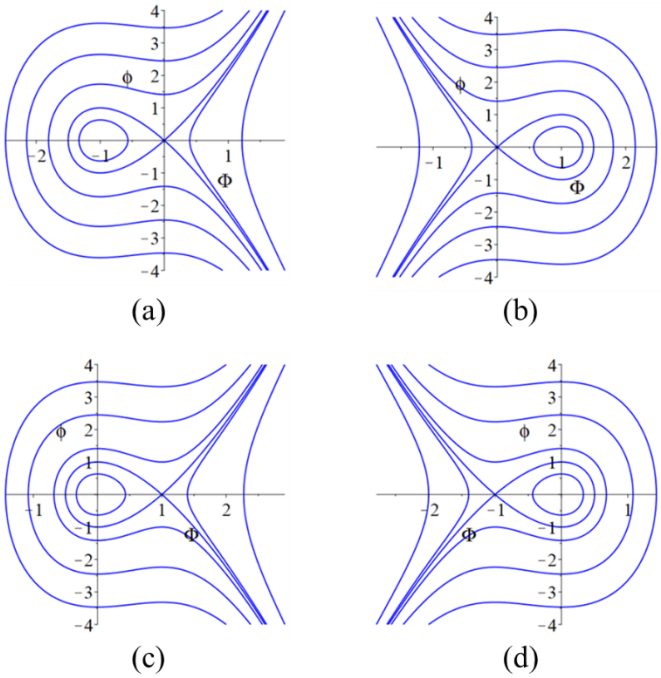

Figure 1. Phase portraits of the PDS.

3.2. Existence conditions of the wave solutions

According to the theory of PDS, the periodic, bell shape, kink solitary, and unbounded traveling wave solutions correspond to the closed, homoclinic, heteroclinic, and opened orbits, respectively. Thus we can conclude

(1) For $\varsigma_1>0$ and $\varsigma_2>0$, Eq (2.6) has the periodic and bell shape wave solutions (see Figure 1(a)).

(2) For $\varsigma_1>0$ and $\varsigma_2<0$, Eq (2.6) has the periodic and bell shape wave solutions (see Figure 1(b)).

(3) For $\varsigma_1<0$ and $\varsigma_2>0$, Eq (2.6) has the periodic and bell shape wave solutions (see Figure 1(c)).

(4) For $\varsigma_1<0$ and $\varsigma_2<0$, Eq (2.6) has the periodic and bell shape wave solutions (see Figure 1(d)).

3.3. *The chaotic performances*

The goal of this section is to study the chaotic performances of the PDS by imposing a

perturbed term as [45]

$$\begin{cases} \dfrac{d\Phi}{d\vartheta} = \phi \\ \dfrac{d\phi}{d\vartheta} = \varsigma_1 \Phi(\vartheta) + \varsigma_2 \Phi^2(\vartheta) + \Psi \sin(\Theta\vartheta) \end{cases}, \tag{19}$$

where Ψ and Θ represent the amplitude and frequency, respectively. In Eq (19), the parameters ς_1, ς_2, Ψ, and Θ may affect the dynamical behaviors of the system. To discuss the effect, we choose the parameters $m=-1$, $\omega=-3$, the time series plot, 2D and 3D phase portraits under the initial conditions $\Phi(0)=0.1$ and $\phi(0)=0$, with the different Θ and Ψ displayed in Figure 2, where (a,b,c) for $\Psi=0.04$, $\Theta=0.03$, (d,e,f) for $\Psi=0.4$, $\Theta=0.3$. We can find that the system is quasi-periodic for $\Psi=0.04$, $\Theta=0.03$; however, it becomes chaotic when $\Psi=0.4$ and $\Theta=0.3$.

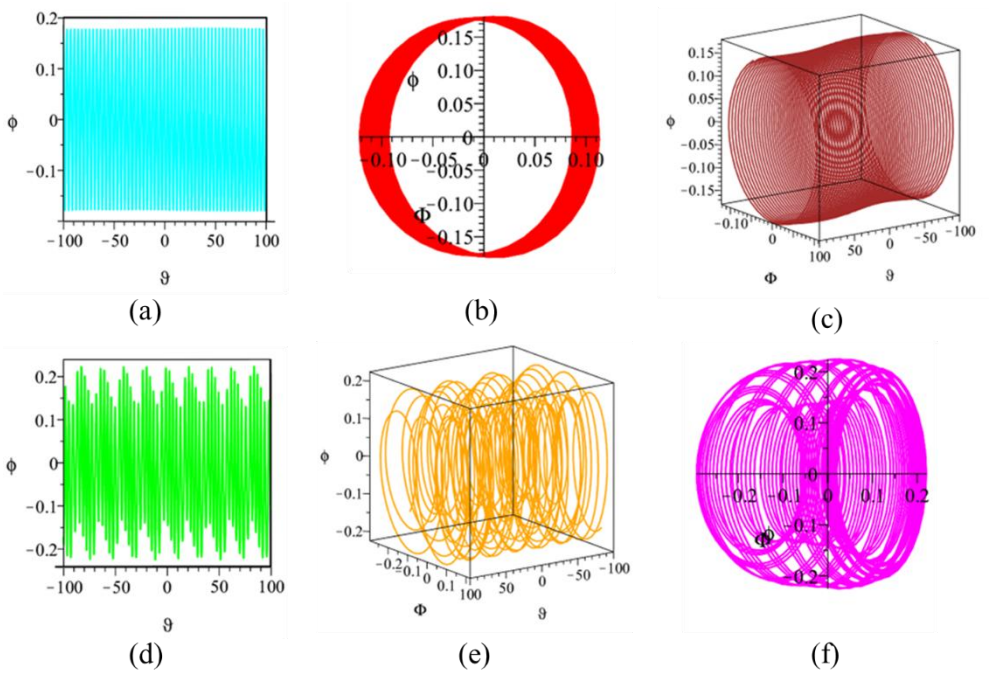

Figure 2. The quasi-periodic and chaotic behaviors with $m=-1$, $\omega=-3$ under the initial conditions $\Phi(0)=0.1$ and $\phi(0)=0$.

3.4. The sensitivity analysis

The major goal of this section is to probe the system through the frequency-amplitude formulation for $m=-1$, $\omega=-1$ at the initial conditions (a) $\Phi(0)=0.2$, $\phi(0)=0.1$, (b) $\Phi(0)=0.25$, $\phi(0)=0.15$, (c) $\Phi(0)=0.2$, $\phi(0)=0.12$ and (d) $\Phi(0)=0.3$, $\phi(0)=0.1$. The comparison results in Figure 3 indicate that minor changes to the initial conditions can impact the behaviors of the solution.

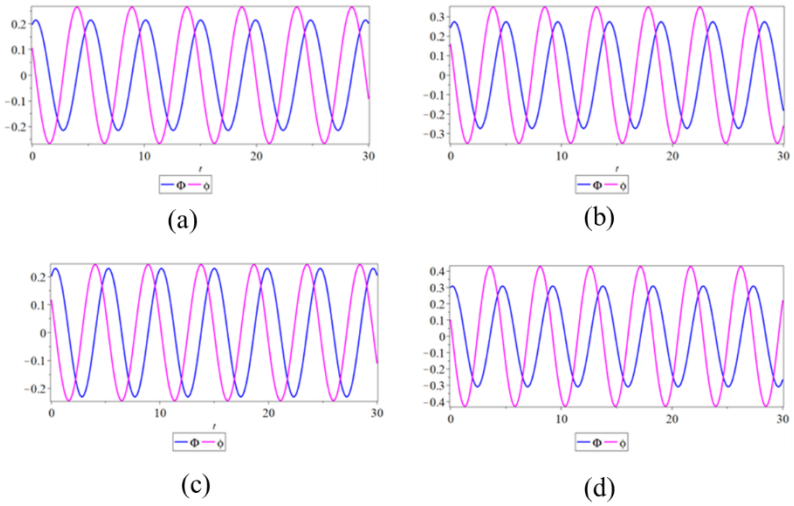

Figure 3. Sensitive analysis of the PDS with $m=-1$, $\omega=-1$ for the different initial conditions.

4. The different wave solutions

In this section, we aim to employ the IAC approach, DMM, and the HBM to develop the abundant wave solutions.

4.1. Application of the IAC approach

4.1.1. The IAC approach

Based on the IAC approach [46–48], considering the following PDS

$$\begin{cases} \xi' = \zeta \\ \zeta' = -a\xi(\vartheta) + b\xi^2(\vartheta) \end{cases}, \tag{20}$$

where $a,b \in R$, $b \neq 0$, and the IAC

$$g(\xi,\zeta) = \frac{1}{2}\zeta^2 + \frac{1}{2}a\xi^2 - \frac{1}{3}b\xi^3 = 0. \tag{21}$$

Theorem 1. The PDS in Eq (20) with the IAC of Eq (21) admits the following results [47,48]

(1) For $a=0$, $g=0$, the solution is

$$\xi(\vartheta) = \frac{12}{2b\vartheta^2 \pm 2\sqrt{6b}\vartheta c_0 + 3c_0^2}. \tag{22}$$

(2) For $a \neq 0$, $a<0$, $g=0$, the solution is

$$\xi(\vartheta) = \frac{3a}{2b}\operatorname{sech}^2\left[\frac{\sqrt{-a}}{2}\left(\vartheta \pm \sqrt{3}c_0\right)\right]. \tag{23}$$

(3) For $a \neq 0$, $a > 0$, $g = 0$, the solution is

$$\xi(\vartheta) = \frac{a}{2b}\left\{-1 + 3\tanh^2\left[\frac{\sqrt{a}}{2}\left(\vartheta \pm \sqrt{3}bc_0\right)\right]\right\}. \tag{24}$$

4.2.2. Application

Based on the PDS in Eq (13), we can get the following IAC

$$g(\phi, \Phi) = \frac{1}{2}(\phi)^2 - \frac{1}{2}\varsigma_1\Phi^2 - \frac{1}{3}\varsigma_2\Phi^3 = 0, \tag{25}$$

where $\varsigma_1 = -\frac{\omega}{m^3}, \varsigma_2 = \frac{3}{m}$. By the IAC approach, comparing Eq (21) with Eq (25) yields

$$a = -\varsigma_1, \tag{26}$$

and

$$b = \varsigma_2. \tag{27}$$

In light of Theorem 1, we can disclose the expressions of Φ through one step as

Case 1: When $\frac{\omega}{m^3} = 0$, we obtain the rational wave solution as

$$\Phi(\vartheta) = \frac{4m}{2\vartheta^2 \pm 2m\sqrt{2m}\vartheta c_0 + mc_0^2}. \tag{28}$$

Integrating it once and setting the integral constant as zero yields

$$\Xi(\vartheta) = \frac{2m\left[2\vartheta \pm \sqrt{2m}c_0\right]}{mc_0^2 - 2\vartheta^2}. \tag{29}$$

So we have:

$$U(x, y, t) = \frac{2m\left[2(mx + ny + \omega t) \pm \sqrt{3m}c_0\right]}{mc_0^2 - 2(mx + ny + \omega t)^2}. \tag{30}$$

Since $\omega \neq 0$, this solution does not exist.

Case 2: When $\frac{\omega}{m^3} < 0$, we can get the bell shape wave solution as

$$\Phi(\vartheta) = \frac{\omega}{2m^2}\operatorname{sech}^2\left[\frac{1}{2}\sqrt{-\frac{\omega}{m^3}}\left(\vartheta \pm \sqrt{3}c_0\right)\right]. \tag{31}$$

Obviously, this solution matches with discussion in section 3.2. Integrating Eq (31) once, we have

$$\Xi(\vartheta) = -\sqrt{\frac{\omega}{m}}\tanh\left[\frac{1}{2}\sqrt{-\frac{\omega}{m^3}}\left(\vartheta \pm \sqrt{3}c_0\right)\right]. \tag{32}$$

So we obtain the kink wave solution as

$$U_{\pm}(x,y,t)=-\sqrt{-\frac{\omega}{m}}\tanh\left[\frac{1}{2}\sqrt{-\frac{\omega}{m^3}}\left(mx+ny+\omega t\pm\sqrt{3}c_0\right)\right]. \tag{33}$$

Case 3: When $\frac{\omega}{m^3}>0$, we can get the periodic wave solution as

$$\Phi(\vartheta)=\frac{\omega}{2m^2}\left\{-1+3\tanh^2\left[\frac{1}{2}\sqrt{\frac{\omega}{m^3}}\left(\vartheta\mp\frac{3\sqrt{3}}{m}c_0\right)\right]\right\}. \tag{34}$$

Obviously, this periodic solution also agrees well with the discussion in section 3.2. Integrating it once and letting the integral constant as zero yields

$$\Xi(\vartheta)=\frac{\omega\vartheta}{m^2}-3\sqrt{\frac{2\omega}{m}}\tanh\left[\frac{1}{2}\sqrt{\frac{\omega}{2m^3}}\left(\vartheta\mp\frac{3\sqrt{3}}{m}c_0\right)\right]. \tag{35}$$

So there is:

$$U_{\pm}(x,y,t)=\frac{\omega(mx+ny+\omega t)}{m^2}-3\sqrt{\frac{2\omega}{m}}\tanh\left[\frac{1}{2}\sqrt{\frac{\omega}{2m^3}}\left(mx+ny+\omega t\mp\frac{3\sqrt{3}}{m}c_0\right)\right]. \tag{36}$$

4.2. Application of the DMM

4.2.1. The DMM

The main steps of the DMM that are based on the unified equation are given as follows
Considering the unified equation with the following form [49]

$$\mu'=\varepsilon\sqrt{c_0+c_1\mu+c_2\mu^2+c_3\mu^3}\,, \tag{37}$$

where $\varepsilon=\pm1$, Equation (37) admits the following different solutions

Case 1: For $c_1=c_0=0$, $c_2>0$, Eq (30) admits a bell-shape wave solution as

$$\mu=-\frac{c_2}{c_3}\operatorname{sech}^2\left(\frac{\sqrt{c_2}}{2}\vartheta\right). \tag{38}$$

Case 2: For $c_1=c_0=0$, $c_2<0$, Eq (30) admits a singular periodic wave solution as

$$\mu=-\frac{c_2}{c_3}\sec^2\left(\frac{\sqrt{-c_2}}{2}\vartheta\right). \tag{39}$$

Case 3: For $c_1 = c_0 = 0$, $c_2 = 0$, Eq (30) admits a rational wave solution as

$$\mu = \frac{4}{c_3 \vartheta^2}. \tag{40}$$

4.2.2. Application

By Eq (7), we have

$$(\Phi')^2 - \frac{2}{m}\Phi^3 + \frac{\omega}{m^3}\Phi^2 = 0, \tag{41}$$

which is

$$\Phi' = \varepsilon\sqrt{-\frac{\omega}{m^3}\Phi^2 + \frac{2}{m}\Phi^3}, \tag{42}$$

where $\varepsilon = \pm 1$. Comparing it with Eq (37) yields

$$c_1 = c_0 = 0, \quad c_2 = -\frac{\omega}{m^3}, \quad c_3 = \frac{2}{m}. \tag{43}$$

Thus we have the following

Case 1: For $\frac{\omega}{m^3} < 0$, Eq (7) admits a bell-shape wave solution as

$$\Phi = \frac{\omega}{2m^2}\operatorname{sech}^2\left(\frac{1}{2}\sqrt{-\frac{\omega}{m^3}}\vartheta\right). \tag{44}$$

This wave solution corresponds to the discussion in section 3.2. In the same way, integrating Eq (44) once and setting the integral constant to zero yields

$$\Xi(\vartheta) = -\sqrt{-\frac{\omega}{m}}\tanh\left(\frac{1}{2}\sqrt{-\frac{\omega}{m^3}}\vartheta\right). \tag{45}$$

Then, the kink wave solution of Eq (1) is

$$U(x,y,t) = -\sqrt{-\frac{\omega}{m}}\tanh\left[\frac{1}{2}\sqrt{-\frac{\omega}{m^3}}(mx + ny + \omega t)\right], \tag{46}$$

which is the same with Eq (33) for $c_0 = 0$. This strongly demonstrates the correctness of the methods used.

Case 2: For $\frac{\omega}{m^3} > 0$, Eq (7) admits a singular periodic solution as

$$\Phi = \frac{\omega}{2m^2}\sec^2\left(\frac{1}{2}\sqrt{\frac{\omega}{m^3}}\vartheta\right), \tag{47}$$

which also corresponds to the discussion in section 3.2. Then we have

$$\Xi = \sqrt{\frac{\omega}{m}}\tan\left(\frac{1}{2}\sqrt{\frac{\omega}{m^3}}\vartheta\right). \tag{48}$$

So, we have the singular periodic wave solution as

$$U(x,y,t) = \sqrt{\frac{\omega}{m}}\tan\left[\frac{1}{2}\sqrt{\frac{\omega}{m^3}}(mx+ny+\omega t)\right]. \tag{49}$$

Case 3: For $\frac{\omega}{m^3} = 0$, Eq (7) admits a rational wave solution as

$$\Phi = \frac{2m}{\vartheta^2}, \tag{50}$$

which is the same as Eq (29) for $c_0 = 0$. This also reveals the correctness of the methods used. Then we have

$$\Xi = -\frac{2m}{\vartheta}. \tag{51}$$

Then there is

$$U(x,y,t) = \frac{2m}{-(mx+ny+\omega t)}. \tag{52}$$

Since $\omega \neq 0$, this solution does not exist.

4.3. Application of the HBM

4.3.1. The HBM

To explore the ODE as

$$\psi'' + f(\psi) = 0. \tag{53}$$

The VP can be found via the SIM as

$$J(\psi) = \int_0^\infty \left\{\frac{1}{2}(\psi')^2 + P(\psi)\right\} d\vartheta, \tag{54}$$

which can be expressed as

$$J(\psi)=\int_0^{\infty}\left\{\frac{1}{2}(\psi')^2+P(\psi)\right\}d\vartheta=\int_0^{\infty}\{D-L\}d\vartheta. \tag{55}$$

The system's Hamiltonian is

$$\mathrm{H}=D+L=\frac{1}{2}(\psi')^2-P(\psi). \tag{56}$$

In the view of the HBM, the periodic solution of Eq (5) can be considered as

$$\psi=\Delta\cos(\Omega\vartheta),\ \ \Omega>0, \tag{57}$$

where Δ represents the amplitude, and Ω is the frequency. We know that the system's total energy should remain unchanged, which is

$$H=D+L=\frac{1}{2}(\psi')^2-P(\psi)=H_0, \tag{58}$$

where H_0 stands for the Hamiltonian constant.

Substituting the initial conditions of Eq (57) into Eq (58), it yields

$$H=D+L=-P(\Delta)=H_0. \tag{59}$$

Inserting Eq (57) into Eq (58) and setting [50]

$$\Omega\vartheta=\frac{\pi}{4}. \tag{60}$$

Then, we obtain the solution through computing the obtained results.

4.3.2. The application

In section 2, we have the Hamiltonian as

$$\mathrm{H}=D+L=\frac{1}{2}(\Phi')^2-\frac{1}{m}\Phi^3+\frac{\omega}{2m^3}\Phi^2. \tag{61}$$

We set:

$$\Phi=\Delta\cos(\Omega\vartheta),\ \ \Omega>0, \tag{62}$$

with the initial conditions as

$$\Phi(0)=\Delta,\ \ \Phi'(0)=0. \tag{63}$$

Substituting them into Eq (61), it yields

$$-\frac{1}{m}\Delta^3+\frac{\omega}{2m^3}\Delta^2=\mathrm{H}_0. \tag{64}$$

Taking Eq (62) into Eq (61) gives

$$\begin{aligned}\mathrm{H} = D + L &= \frac{1}{2}\left[-\Delta\Omega\sin s(\Omega\vartheta)\right]^2 - \frac{1}{m}\left[\Delta\cos(\Omega\vartheta)\right]^3 + \frac{\omega}{2m^3}\left[\Delta\cos(\Omega\vartheta)\right]^2 \\ &= -\frac{1}{m}\Delta^3 + \frac{\omega}{2m^3}\Delta^2 = \mathrm{H}_0\end{aligned}. \tag{65}$$

Letting

$$\Omega\vartheta = \frac{\pi}{4}. \tag{66}$$

We have

$$\frac{1}{2}\left[-\frac{\sqrt{2}}{2}\Delta\Omega\right]^2 - \frac{1}{m}\left[\frac{\sqrt{2}}{2}\Delta\right]^3 + \frac{\omega}{2m^3}\left[\frac{\sqrt{2}}{2}\Delta\right]^2 = -\frac{1}{m}\Delta^3 + \frac{\omega}{2m^3}\Delta^2. \tag{67}$$

Solving it, yields

$$\Omega = \sqrt{\frac{\left(\sqrt{2}-4\right)\Delta}{m} + \frac{\omega}{m^3}}. \tag{68}$$

Then, we have the periodic solution as

$$\Phi = \Delta\cos\left(\sqrt{\frac{\left(\sqrt{2}-4\right)\Delta}{m} + \frac{\omega}{m^3}}\vartheta\right), \tag{69}$$

which is consistent with the discussion in section 3.2. Then, we have

$$\Xi = \frac{\Delta}{\sqrt{\frac{\left(\sqrt{2}-4\right)\Delta}{m} + \frac{\omega}{m^3}}}\sin\left(\sqrt{\frac{\left(\sqrt{2}-4\right)\Delta}{m} + \frac{\omega}{m^3}}\vartheta\right). \tag{70}$$

So there is:

$$U(x,y,t) = \frac{\Delta}{\sqrt{\frac{\left(\sqrt{2}-4\right)\Delta}{m} + \frac{\omega}{m^3}}}\sin\left[\sqrt{\frac{\left(\sqrt{2}-4\right)\Delta}{m} + \frac{\omega}{m^3}}(mx + ny + \omega t)\right]. \tag{71}$$

5. Results and discussions

The goal of this section is to discuss and present the results obtained in section 4.

Assigning the parameters as $m=1$, $n=2$, $\omega=-3$, $c_0=1$, the shapes of Eq (36) on the interval $x\in[-5,5]$ and $y\in[-5,5]$ at $t=0$ are shown in Figure 4. The wave is the anti-kink solitary wave.

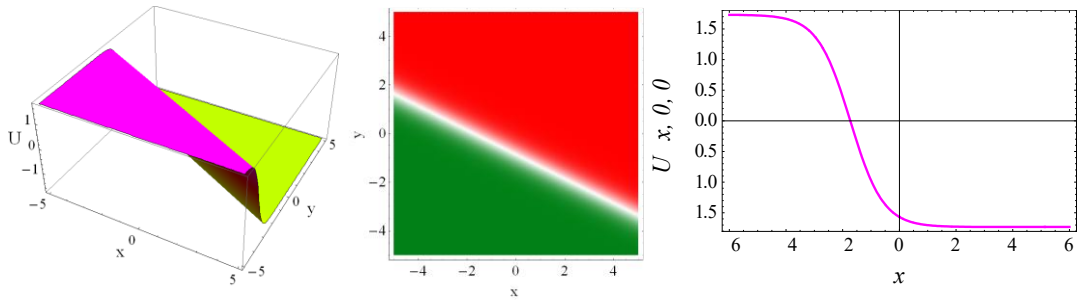

(a) (b) (c)

Figure 4. Outlines of Eq (36) with $m=1$, $n=2$, $\omega=-3$, $c_0=1$.

If we select $m=1$, $n=2$, $\omega=1$, the outlines of Eq (46) on the interval $x\in[-5,5]$ and $y\in[-5,5]$ for $t=0$ are displayed in Figure 5. It can be seen that the wave is the kink solitary wave.

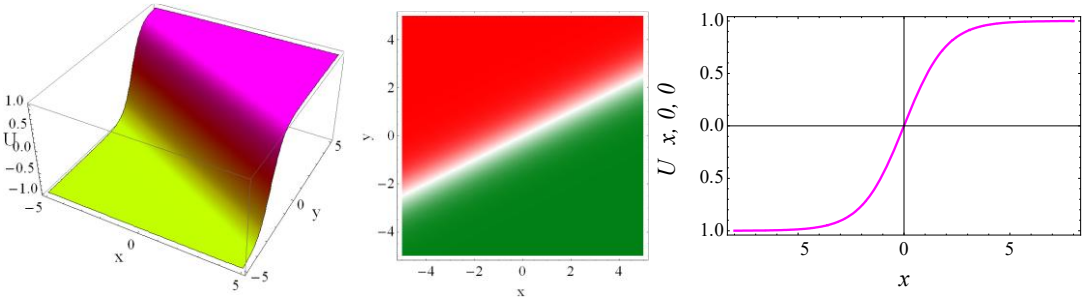

(a) (b) (c)

Figure 5. Outlines of Eq (46) with $m=1$, $n=2$, $\omega=1$.

Figure 6 presents the shapes of Eq (49) on the interval $x\in[-8,8]$ and $y\in[-8,8]$ for $t=0$ with the parameters as $m=-1$, $n=1$, $\omega=1$. Here, the wave structure is the singular periodic wave.

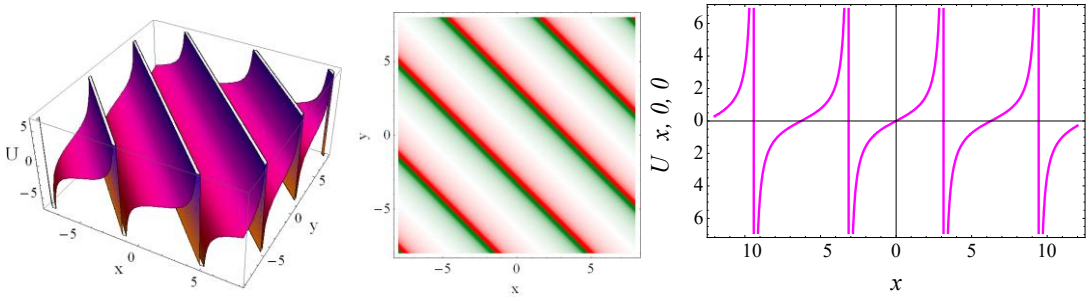

(a) (b) (c)

Figure 6. Outlines of Eq (49) with $\alpha=1$, $\beta=1$, $\gamma=1$, $\vartheta=1$.

When the parameters are used as $\Delta = 1$ $m = 1$, $n = 2$, $\omega = 3$, the performances of Eq (71) are revealed in Figure 7. It can be seen that the wave is a periodic wave.

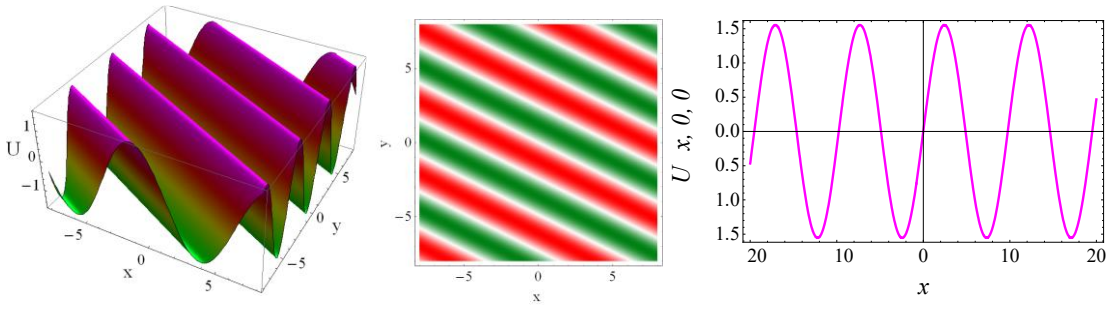

(a) (b) (c)

Figure 7. Outlines of Eq (71) with $\Delta = 1$, $m = 1$, $n = 2$, $\omega = 3$.

6. Conclusions

The (2+1)-dimensional BLMPE equation has been explored qualitatively and quantitatively in this research. The VP and Hamiltonian were developed with the aid of the travelling wave transformation and SIM. Then, the PDS was derived, and the phase portraits and the bifurcation study were presented to discuss the existence conditions of the solutions with the different structures. Besides, the chaotic behaviors and the sensitivity analysis were also elaborated. In the end, three effective methods, the IAC approach, DMM, and the HBM, were employed to probe the different wave solutions, including the kink solitary, anti-kink solitary, singular periodic, and periodic wave solutions. The profiles of the obtained solutions are displayed graphically by selecting the appropriate parameter values. As far as we know, the results in this work were all new and can help us gain a deeper understanding of the dynamics of the (2+1)-dimensional BLMPE equation. In addition, the methods used in this paper were not all based on the symbolic computation; instead, they are more direct, and simple, and can avoid complex calculation processes, allowing them to be employed to probe the solutions of other NPDEs.

Author contributions

Kangjia Wang: Conceptualization, Methodology, Software, Validation, Formal analysis, Writing-review and editing, Visualization; Kanghua Yan: Conceptualization, Writing-review and editing; Feng Shi: Conceptualization, Methodology, Software, Writing-original draft preparation, Writing-review; Geng Li: Software, Validation; Xiaolian Liu: Software, Validation, Writing-review. All authors have read and approved the final version of the manuscript for publication.

Use of Generative-AI tools declaration

The authors declare they have not used Artificial Intelligence (AI) tools in the creation of this article.

Conflict of interest

The authors declare that they have no known competing financial interests or personal relationships that could have appeared to influence the work reported in this paper.

References

1. Y. Zhu, J. Yang, J Li, L. Hu, Q. Zhou, Interaction properties of double-hump solitons in the dispersion decreasing fiber, *Nonlinear Dyn.*, **109** (2022), 1047–1052. https://doi.org/10.1007/s11071-022-07491-7
2. J. Yang, Y. Zhu, W. Qin, S. H. Wang, C. Q. Dai, J. T. Li, Higher-dimensional soliton structures of a variable-coefficient Gross-Pitaevskii equation with the partially nonlocal nonlinearity under a harmonic potential, *Nonlinear Dyn.*, **108** (2022), 2551–2562. https://doi.org/10.1007/s11071-022-07337-2
3. M. M. Roshid, H. Or-Roshid, Effect of the nonlinear dispersive coefficient on time-dependent variable coefficient soliton solutions of the Kolmogorov-Petrovsky-Piskunov model arising in biological and chemical science, *Heliyon*, **10** (2024), e31294. https://doi.org/10.1016/j.heliyon.2024.e31294
4. X. Lü, H. Hui, F. Liu, Y. Bai, Stability and optimal control strategies for a novel epidemic model of COVID-19, *Nonlinear Dyn.*, **106** (2021), 1491–1507. https://doi.org/10.1007/s11071-021-06524-x
5. S. Duran, An investigation of the physical dynamics of a traveling wave solution called a bright soliton, *Phys. Scr.*, **96** (2021), 125251. https://doi.org/10.1088/1402-4896/ac37a1
6. K. J Wang, S. Li, K. H. Yan, Resonant multiple wave, multi-lump wave and complex N-soliton solutions to the (3+1)-dimensional Jimbo-Miwa equation, *Mod. Phys. Lett. B*, **40** (2026), 265000. https://doi.org/10.1142/S0217984926500016
7. Y. S. Özkan, E. Yaşar, Breather-type and multi-wave solutions for (2+1)-dimensional nonlocal Gardner equation, *Appl. Math. Comput.*, **390** (2021), 125663. https://doi.org/10.1016/j.amc.2020.125663
8. Y. Sağlam Özkan, A. R. Seadawy, E. Yaşar, Multi-wave, breather and interaction solutions to (3+1) dimensional Vakhnenko-Parkes equation arising at propagation of high-frequency waves in a relaxing medium, *J. Taibah Uni. Sci.*, **15** (2021), 666–678. https://doi.org/10.1080/16583655.2021.1999053
9. Y. H Liang, K. J. Wang, Dynamics of the new exact wave solutions to the local fractional Vakhnenko-Parkes equation, *Fractal*, **33** (2025), 2550102. https://doi.org/10.1142/S0218348X25501026
10. S. Kumar, K. Singh, R. K. Gupta, Coupled Higgs field equation and Hamiltonian amplitude equation: Lie classical approach and (G'/G)-expansion method, *Pramana*, **79** (2012), 41–60. https://doi.org/10.1007/s12043-012-0284-7
11. A. Malik, F. Chand, H. Kumar, Exact solutions of some physical models using the (G'/G)-expansion method, *Pramana*, **78** (2012), 513–529. https://doi.org/10.1007/s12043-011-0253-6

12. W. X. Ma, J. H. Lee, A transformed rational function method and exact solutions to the 3+1 dimensional Jimbo-Miwa equation, *Chaos Solitons Fract.,* **42** (2009), 1356–1363. https://doi.org/10.1016/j.chaos.2009.03.043
13. Y. X. Ma, B. Tian, Q. X. Qu, Painlevé analysis, Bäcklund transformations and traveling-wave solutions for a (3+1)-dimensional generalized Kadomtsev-Petviashvili equation in a fluid, *Int. J. Mod. Phys. B*, **35** (2021), 2150108. https://doi.org/10.1142/S0217979221501083
14. P. F. Han, T. Bao, Bäcklund transformation and some different types of N-soliton solutions to the (3+1)-dimensional generalized nonlinear evolution equation for the shallow-water waves, *Math. Meth. Appl. Sci.*, **44** (2021), 11307–11323. https://doi.org/10.1002/mma.7490
15. D. Shang, Exact solutions of coupled nonlinear Klein-Gordon equation, *Appl. Math. Comput.*, **217** (2010), 1577–1583. https://doi.org/10.1016/j.amc.2009.06.072
16. E. M. E. Zayed, K. A. Gepreel, M. El-Horbaty, Optical solitons in birefringent fibers with Kaup-Newell equation using two integration schemes, *Optik*, **251** (2022), 167992. https://doi.org/10.1016/j.ijleo.2021.167992
17. W. B. Rabie, H. M. Ahmed, Dynamical solitons and other solutions for nonlinear Biswas–Milovic equation with Kudryashov's law by improved modified extended tanh-function method, *Optik*, **245** (2021), 167665. https://doi.org/10.1016/j.ijleo.2021.167665
18. X. Wang, J. Wu, Y. Wang, C. Chen, Extended tanh-function method and its applications in nonlocal complex mKdV equations, *Mathematics*, **10** (2022), 3250. https://doi.org/10.3390/math10183250
19. A. Zulfiqar, J. Ahmad, Soliton solutions of fractional modified unstable Schrödinger equation using Exp-function method, *Results Phys.*, **19** (2020), 103476. https://doi.org/10.1016/j.rinp.2020.103476
20. S. T. Mohyud-Din, Y. Khan, N. Faraz, Exp-function method for solitary and periodic solutions of Fitzhugh-Nagumo equation, *Int. J. Numer. Meth. Heat Fluid Flow*, **22** (2012), 335–341. https://doi.org/10.1108/09615531211208042
21. U. Afzal, N. Raza, N, I. G. Murtaza, On soliton solutions of time fractional form of Sawada-Kotera equation, *Nonlinear Dyn.,* **95** (2019), 391–405. https://doi.org/10.1007/s11071-018-4571-9
22. N. Raza, A. Javid, Optical dark and dark-singular soliton solutions of (1+2)-dimensional chiral nonlinear Schrodinger' s equation, *Waves Rand. Complex Media*, **29** (2019), 496–508. https://doi.org/10.1080/17455030.2018.1451009
23. T. Wang, L. Tian, Z. Ma, Z. Yang, H. Han, Bifurcation soliton solutions, M-lump, breather waves, and interaction solutions for (3+1)-dimensional P-type equation, *Chaos Solitons Fract.,* **192** (2025), 115932. https://doi.org/10.1016/j.chaos.2024.115932
24. Z. Ma, H. Han, L. Tian, Multiple solitons, multiple lump solutions, and lump wave with solitons for a novel (2+1)-dimensional nonlinear partial differential equation, *Phys. Scr.*, **99** (2024), 115238. https://doi.org/10.1088/1402-4896/ad831b
25. M. A. Abdou, The extended F-expansion method and its application for a class of nonlinear evolution equations, *Chaos Solitons Fractals*, **31** (2017), 95–104. https://doi.org/10.1016/j.chaos.2005.09.030
26. W. B. Rabie, H. M. Ahmed, Cubic-quartic optical solitons and other solutions for twin-core couplers with polynomial law of nonlinearity using the extended F-expansion method, *Optik*, **253** (2022), 168575. https://doi.org/10.1016/j.ijleo.2022.168575

27. X. Guan, W. Liu, Q. Zhou, Darboux transformation and analytic solutions for a generalized super-NLS-mKdV equation, *Nonlinear Dyn.*, **98** (2019), 1491–1500. https://doi.org/10.1007/s11071-019-05275-0
28. J. Yang, Y. Zhu, W. Qin, 3D bright-bright Peregrine triple-one structures in a nonautonomous partially nonlocal vector nonlinear Schrödinger model under a harmonic potential, *Nonlinear Dyn.*, **111**(2023), 13287–13296. https://doi.org/10.1007/s11071-023-08526-3
29. F. Bouzari Liavoli, A. Fakharian, H. Khaloozadeh, Sub-optimal controller design for time-delay nonlinear partial differential equation systems: An extended state-dependent differential Riccati equation approach, *Int. J. Syst. Sci.,* **54** (2023), 1815–1840. https://doi.org/10.1080/00207721.2023.2210140
30. W. W. Mohammed, A. M. Albalahi, S. Albadrani, E. S. Aly, R. Sidaoui, A. E. Matouk, The analytical solutions of the stochastic fractional Kuramoto-Sivashinsky equation by using the Riccati equation method, *Math. Prob. Eng.*, **2022** (2022), 5083784. https://doi.org/10.1155/2022/5083784
31. B. Chen, Z. Ma, Y. Liu, Q. Bi, Lump solution, lump and soliton interaction solution, breather solution, and interference wave solution for the (3+1)-dimensional fourth-order nonlinear equation by bilinear neural network method, *Mod. Phys. Lett. B*, **39** (2025), 2550143. https://doi.org/10.1142/S021798492550143X
32. Z. Ma, Y. Liu, Y. Wang, The exact analytical solutions of the (2+1)-dimensional extended Korteweg-de Vries equation using bilinear neural network method and bilinear residual network method, *Mod. Phys. Lett. B*, **39** (2025), 2550045. https://doi.org/10.1142/S0217984925500459
33. K. L. Wang, Dynamical analysis of the soliton solutions for the nonlinear fractional Akbota equation, *Fractals*, **33** (2025), 2550084. http://doi.org/10.1142/S0218348X25500847
34. K. L. Wang, Diversity of soliton solutions to the nonlinear fractional Kadoma, *Fractals*, **33** (2025), 2550107. http://doi.org/10.1142/S0218348X25501075
35. X. Y. Gao, Incompressible fluid symbolic computation and bäcklund transformation: (3+1)-dimensional variable-coefficient Boiti-Leon-Manna-Pempinelli model, *Zeitschrift Naturforschung A*, **70** (2025), 59–61. https://doi.org/10.1515/zna-2014-0272
36. Y. Tang, W. Zai, New periodic-wave solutions for (2+1) and (3+1)-dimensional Boiti-Leon-Manna-Pempinelli equations, *Nonlinear Dyn.*, **81** (2015), 249–255. https://doi.org/10.1007/s11071-015-1986-4
37. M. T. A. Darvishi, M. Najafi, L. C. Kavitha, Stair and step soliton solutions of the integrable (2+ 1) and (3+ 1)-dimensional Boiti-Leon-Manna-Pempinelli equations, *Commun. Theoret. Phys.*, **58** (2012), 785. https://doi.org/10.1088/0253-6102/58/6/01
38. K. J. Wang, F. Shi, Multi-soliton solutions and soliton molecules of the (2+1)-dimensional Boiti-Leon-Manna-Pempinelli equation for the incompressible fluid, *EPL*, **145** (2024), 42001. https://doi.org/10.1209/0295-5075/ad219d
39. L. Hu, Y. T. Gao, S. L. Jia, J. J. Su, G. F. Deng, Solitons for the (2+1)-dimensional Boiti-Leon-Manna-Pempinelli equation for an irrotational incompressible fluid via the Pfaffian technique, *Mod. Phys. Lett. B*, **33** (2019), 1950376. https://doi.org/10.1142/S0217984919503767
40. Y. F. He, Multi-lump, Resonant Y-shape soliton, complex multi kink solitons and the solitary wave solutions to the (2+1)-dimensional Boiti-Leon-Manna-Pempinelli equation for incompressible fluid, *Phys. Scr.*, **99** (2024), 095201. https://doi.org/10.1088/1402-4896/ad664a

41. A. R. Seadawy, A. Ali, M. A. Helal, Analytical wave solutions of the (2+1)-dimensional Boiti-Leon-Pempinelli and Boiti-Leon-Manna-Pempinelli equations by mathematical methods, *Math. Meth. Appl. Sci.*, **44** (2021), 14292–14315. https://doi.org/10.1002/mma.7697
42. M. Najafi, S. Arbabi, M. Najafi, Wronskian determinant solutions of the (2+1)-dimensional Boiti-Leon-Manna-Pempinelli equation, *Int. J. Adv. Math. Sci*, **1** (2013), 8–11. https://doi.org/10.4236/jamp.2013.15004
43. J. H. He, Semi-Inverse method of establishing generalized variational principles for fluid mechanics with emphasis on turbomachinery aerodynamics, *Int. J. Turbo Jet Engines*, **14** (1997), 23–28. https://doi.org/10.1515/TJJ.1997.14.1.23
44. K. J. Wang, K. H. Yan, S. Li, G. Li, A variational principle of the complex Hirota-dynamical model for optics, *Int. J. Mod. Phys. B*, (2025), 2550298. https://doi.org/10.1142/S0217979225502984
45. Y. H. Liang, K. J. Wang, Chaotic pattern, phase portrait, bifurcation analysis, variational principle, Hamiltonian and diverse wave solutions of the generalized (3+1)-dimensional B-type Kadomtsev-Petviashvili equation, *Pramana*, 2026. https://doi.org/10.1007/s12043-025-03057-5
46. A. Gasull, H. Giacomini, Explicit travelling waves and invariant algebraic curves, *Nonlinearity*, **28** (2015), 1597. https://doi.org/10.1088/0951-7715/28/6/1597
47. A. Chen, W. Zhu, Z. Qiao, W. Huang, Algebraic traveling wave solutions of a non-local hydrodynamic-type model, *Math. Phys. Anal. Geom.*, **17** (2014), 465–482. https://doi.org/10.1007/s11040-014-9165-2
48. C. Valls, Algebraic traveling waves for the generalized Newell-Whitehead-Segel equation, *Nonlinear Anal.: Real World Appl.*, **36** (2017), 249–266. https://doi.org/10.1016/j.nonrwa.2017.01.013
49. E. Fan, Multiple travelling wave solutions of nonlinear evolution equations using a unified algebraic method, *J. Phys. A: Math. Gen.*, **35** (2002), 6853. https://doi.org/10.1088/0305-4470/35/32/306
50. J. H. He, Preliminary report on the energy balance for nonlinear oscillations, *Mech. Res. Commun.*, **29** (2002), 107–111. https://doi.org/10.1016/S0093-6413(02)00237-9

AIMS Press